# Analysis of a Wide Compound Slot-Coupled Parallel Waveguide Coupler and Radiator

A. Mohammed Rajeek and Ajay Chakraborty, *Senior Member, IEEE*

*Abstract*—**An analysis of a parallel waveguide coupler coupled through a wide compound slot, offset from center line and inclined with respect to the longitudinal axis of a rectangular waveguide, is presented. The Galerkin method of moments with sinusoidal basis functions is used to solve the slot aperture electric field integral equations, taking into account finite wall thickness. The highly complicated moment matrices are analytically evaluated using a modified geometry of the slot. Compound slot parallel coupler characteristics are then deduced, including resonant length, dominant mode scattering, and the equivalent network. The theoretical results of both the magnitude and phase of the $S$ parameters are compared with the experimental results. The analysis is extended to study a compound slot radiator, and the results are compared with the results available in the literature. Quantitative data on the aperture electric field phase variability of 360° with slot offset and tilt are given for a compound slot radiator. The equivalent circuit of a compound slot radiator, which turns out to be an antisymmetric $T$ network, is also found.**

## I. Introduction

PARALLEL waveguide couplers are useful in feeding a linear slot array, measuring high powers, designing a directional coupler, etc. The treatment of slots in waveguides started with Bethe [1] who developed the theory for very small apertures which was later modified by Cohn [2] for large apertures of finite thickness. The modified Bethe–Cohn theory has been applied to the design of multiaperture couplers by Levy [3]. Watson [4] deduced several approximate equivalent circuit representations for waveguide slot couplers. Among the other methods, a few are the variational technique [5], the method based upon self-reaction [6], and the method of methods [7]–[11], [13], [14].

In a series of papers, Rengarajan has analyzed slot coupling between two waveguides using longitudinal/transverse slots [9], a centered inclined slot [10], and a compound slot [11]. But in all of these cases, the coupling is between two crossed waveguides. An accurate study of coupling between parallel couplers through a slot in the common broad wall is also equally necessary owing to its use in the directional coupler, high-power measurement, etc. In the most recent of these, Datta *et al.* [13] have presented the analysis of a parallel coupler coupled via a longitudinal and transverse slot using Galerkin's method of moments, and the equivalent circuit has been given as a symmetrical $T$ network (predominantly shunt) for a longitudinal slot coupler and a series element for a transverse slot case. The value of equivalent network elements at resonance shows no variation with offset [13]. In this context, it is felt worthwhile to study a more generalized case, wherein the slot in the common broad wall between the parallel coupler is offset from the center as well as inclined, called a compound slot parallel coupler, which is likely to give more degrees of freedom in the design of a multiaperture coupler with a small number of elements.

The analysis of an inclined slot is very complicated. This is even more so in the case of a broad wall compound slot coupler than in a narrow wall coupler [14]. Rengarajan's analysis of compound slots [10], [11], [15] is valid for narrow slots only as he ensures the continuity of tangential magnetic field at the center of the slot only.

In the present work on the compound slot parallel coupler, integral equations for the slot aperture electric field are developed using a dyadic Green's function for the electric vector potential in a waveguide, taking into account the finite wall thickness as a cavity [18], and are solved using Galerkin's method of moments with sinusoidal basis and testing functions defined over the entire region of the slot using a modified geometry [14], making it applicable for wide slots. The scattering parameters, and hence the equivalent network at the plane of symmetry of the slot, have also been found. Theoretical results of $S$ parameters are compared with experimental results for a compound slot parallel coupler.

The analysis of the compound slot coupler is extended to a compound slot radiator, and the results are compared with those in the literature [15]. Also, quantitative data on the variation of the phase of the aperture electric field with inclination and offset are also given, which have been presented only qualitatively in [15]. Also, an equivalent circuit has not been computed in [15], which is also evaluated in the present work, giving better insight into the behavior of the compound slot radiator.

## II. Analysis of Compound Slot Parallel Coupler

### A. Formulation

Fig. 1(a) shows two rectangular waveguides of dimensions $a \times b$ coupled through an offset inclined slot (compound slot) of length "$2L$" and width "$2W$" in the common broad wall between them. Fig. 1(b) shows an enlarged view of the compound slot in the broad wall with the associated local coordinate system and the modified geometry of the slot. Fig. 1(c) shows the longitudinal cross-sectional view of

Manuscript received Feb. 17, 1994; revised July 13, 1994.

The authors are with the Department of Electronics and Electrical Communication Engineering, Indian Institute of Technology, Kharagpur 721302, India.

IEEE Log Number 9408549.

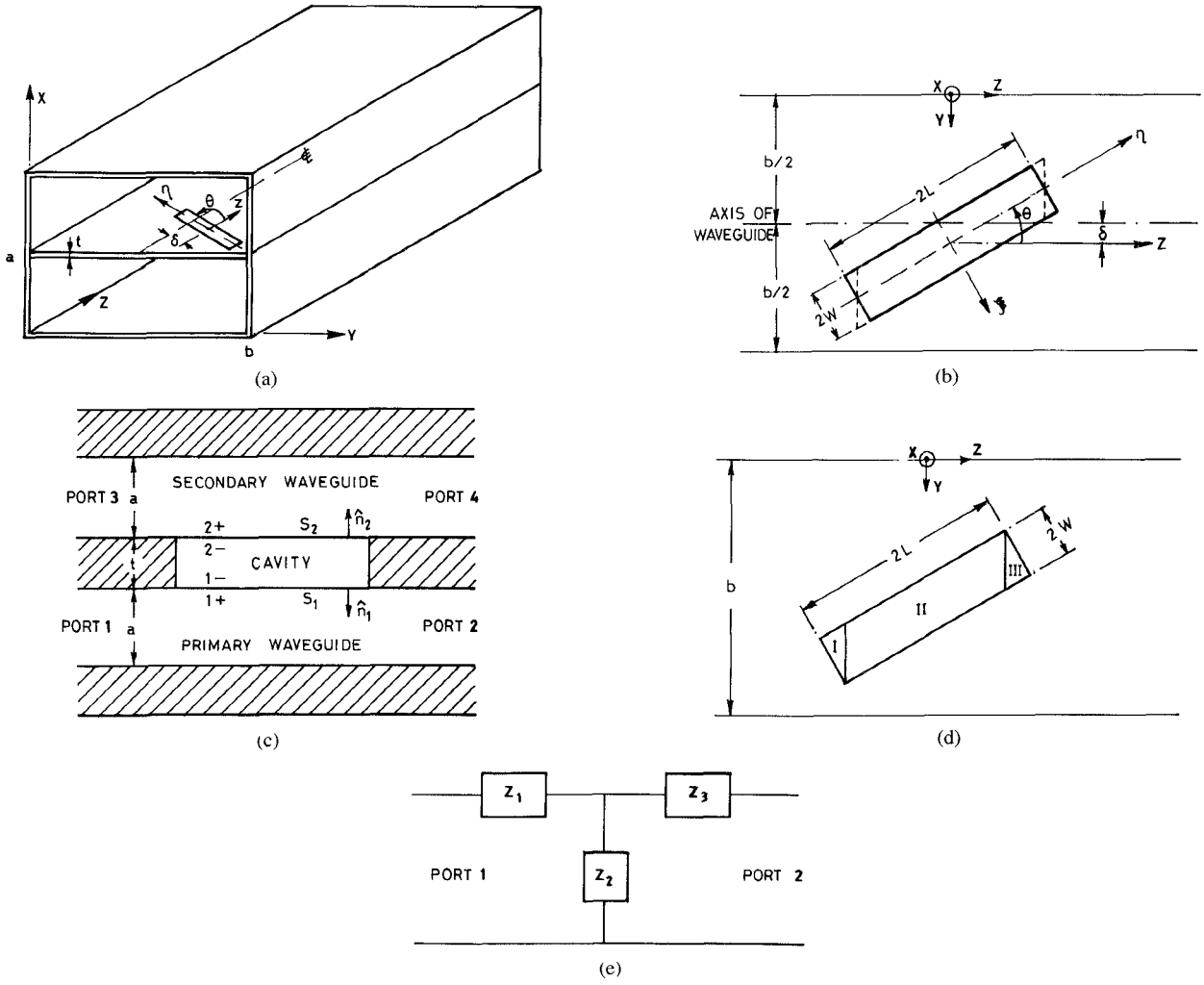


Fig. 1. (a) Two parallel waveguides coupled through a compound slot in the common broad wall between them. (b) Modified geometry of the compound slot with the associated local coordinate system. (c) Enlarged cross-sectional view of coupler showing the finite thickness "$t$" of the waveguide. (d) Enlarged view of compound slot showing the three regions of the actual slot wherein the scattered magnetic field has to be evaluated separately. (e) Equivalent circuit of the coupler at the $z = 0$ plane.

a coupler. The thick slot is treated as a rectangular cavity [18] having dimensions $2L \times 2W \times t$. In the forthcoming analysis, the subscripted variables $(x_0, y_0, z_0, \eta_0, \xi_0)$ are used to denote the source-related variables, and the corresponding unsubscripted ones are for the field-related variables.

The aperture electric field in the lower $(S_1)$ and upper $(S_2)$ interfaces of the slot are expressed using global sinusoidal basis functions as

$$\vec{E}_{S_1} = \hat{\xi}\sum_{q=1}^{N} a_q f_q^1(\eta_0)$$

where

$$f_q^1(\eta_0) = \sin\left\{\frac{q\pi}{2L}(\eta_0 + L)\right\}$$
$$\text{for } -L \le \eta_0 \le L, \; -W \le \xi_0 \le W, \quad \text{and } x_0 = a \quad (1)$$

and

$$\vec{E}_{S_2} = \hat{\xi}\sum_{q=1}^{N} b_q f_q^2(\eta_0)$$

where

$$f_q^2(\eta_0) = \sin\left\{\frac{q\pi}{2L}(\eta_0 + L)\right\}$$
$$\text{for } -L \le \eta_0 \le L, \; -W \le \xi_0 \le W, \quad \text{and } x_0 = a+t. \quad (2)$$

Applying the equivalence principle, the domain of the problem is separated into three regions, viz.

1) primary waveguide with equivalent magnetic current $\vec{M}_{1+}$

2) secondary waveguide with equivalent magnetic current $\vec{M}_{2+}$

3) cavity region with equivalent magnetic currents $\vec{M}_{1-}$ and $\vec{M}_{2-}$ where

$$\vec{M}_{1+} = \vec{E}_{S_1} \times \hat{n}_1 \quad \text{and} \quad \vec{M}_{2+} = \vec{E}_{S_2} \times \hat{n}_2 \quad (3a)$$

$$\vec{M}_{1-} = -\vec{M}_{1+} \quad \text{and} \quad \vec{M}_{2-} = -\vec{M}_{2+} \quad (3b)$$

where $\hat{n}_1$ and $\hat{n}_2$ are unit normal vectors to $S_1$ and $S_2$, as shown in Fig. 1(c).

Ensuring the continuity of the longitudinal components of the magnetic field ($\hat{\eta}$-directed) across the surfaces $S_1$ and $S_2$

results in a pair of coupled integro-differential equations as follows:

$$\sum_{q=1}^{N} a_q[H_\eta^{1+}(f_q^1) + H_\eta^{1-}(f_q^1)] + \sum_{q=1}^{N} b_q H_\eta^{1-}(f_q^2) = -H_\eta^{\text{inc}} \quad (4a)$$

$$\sum_{q=1}^{N} b_q[H_\eta^{2+}(f_q^2) + H_\eta^{2-}(f_q^2)] + \sum_{q=1}^{N} a_q H_\eta^{2-}(f_q^1) = 0 \quad (4b)$$

where

- $H_\eta^{1+}(f_q^i)$ is the $\hat{\eta}$-directed magnetic field at the $i+$ surface (primary/secondary waveguide region) due to the $q$th half sinusoidal variation of the $\hat{\eta}$-directed magnetic current $f_q^i(\eta_0)$ in that surface
- $H_\eta^{i-}(f_q^j)$ is the $\hat{\eta}$-directed magnetic field at the $i-$ surface (cavity region) due to the $q$th half sinusoidal variation of the $\hat{\eta}$-directed magnetic current $f_q^j(\eta_0)$ in the $j$-surface
- $H_\eta^{\text{inc}}$ is the $\hat{\eta}$-directed magnetic field at the $1+$ surface due to the dominant mode excitation of the primary waveguide.

Taking the scalar product of (4a) and (4b) with $f_p^i(\eta)$ and $f_p^2(\eta)$ (for $p = 1$–$N$), respectively, the following set of matrix equations is obtained:

$$\begin{bmatrix} [Y^{\text{int}}] + [Y^{11}] & [Y^{12}] \\ [Y^{21}] & [Y^{\text{ext}}] + [Y^{22}] \end{bmatrix} \begin{bmatrix} [A] \\ [B] \end{bmatrix} = \begin{bmatrix} -[H] \\ [0] \end{bmatrix} \quad (5)$$

where the $(p, q)$th elements of the submatrices appearing in (5) are given by

$$Y_{pq}^{\text{int}} = \int\int_{S_1} f_p^1(\eta) H_\eta^{1+}(f_q^1)\, d\eta\, d\xi \quad (6a)$$

$$Y_{pq}^{\text{ext}} = \int\int_{S_2} f_p^2(\eta) H_\eta^{2+}(f_q^2)\, d\eta\, d\xi \quad (6b)$$

$$Y_{pq}^{ij} = \int\int_{S_1} f_p^i(\eta) H_\eta^{1-}(f_q^j)\, d\eta\, d\xi \quad (6c)$$

$$H_p = \int\int_{S_1} f_p^1(\eta) H_\eta^{\text{inc}}\, d\eta\, d\xi \quad (6d)$$

$$[A] = [a_1\ a_2\ \cdots\ a_N]^T \quad (6e)$$

$$[B] = [b_1\ b_2\ \cdots\ b_N]^T. \quad (6f)$$

The elements of $Y^{ij}$ as given by (6c) are computed using the cavity Green's function approach as given in [18].

### B. Evaluation of $Y^{\text{inc}}$

The magnetic field $\vec{H}$ scattered in a waveguide due to a magnetic source $\vec{M}$ is given by

$$\vec{H} = -j\omega\epsilon\left[\tilde{\tilde{i}} + \frac{\nabla\nabla}{k^2}\right] \cdot \int\int\int_{V_0} \vec{M} \cdot \tilde{\tilde{G}}(r \mid r_0)\, dV_0 \quad (7)$$

where $\tilde{\tilde{G}}(r \mid r_0)$ is the dyadic Green's function for the electric vector potential in a rectangular waveguide given by

$$\tilde{\tilde{G}}(r \mid r_0) = \hat{x}\hat{x}G_{xx} + \hat{y}\hat{y}G_{yy} + \hat{z}\hat{z}G_{zz} = \sum_{m=0}^{\infty}\sum_{n=0}^{\infty} \frac{\epsilon_m \epsilon_n e^{-k_{mn}|z-z_0|}}{2abk_{mn}} \cdot \{\hat{x}\hat{x}S_xC_y + \hat{y}\hat{y}C_xS_y + \hat{z}\hat{z}C_xC_y\} \quad (8)$$

where

$$S_i = \sin(k_i i)\sin(k_i i_0) \quad \text{and} \quad C_i = \cos(k_i i)\cos(k_i i_0)$$

$$k_x = m\pi/a,\ k_y = n\pi/b, \quad \text{and} \quad k_{mn} = [k_x^2 + k_y^2 - k^2]^{0.5}.$$

Using the following transformations between the two coordinates shown in Fig. 1(b)

$$\hat{z} = \hat{\eta}\cos(\theta) + \hat{\xi}\sin(\theta);\ \hat{y} = -\hat{\eta}\sin(\theta) + \hat{\xi}\cos(\theta) \quad (9a)$$

$$z = \eta\cos(\theta) + \xi\sin(\theta);\ y = a/2 + \delta + \xi\cos(\theta) - \eta\sin(\theta) \quad (9b)$$

the $\hat{\eta}$-directed magnetic field appearing in (6a) can be obtained as follows:

$$H_\eta = \mathcal{L}_1(F_\eta) + \mathcal{L}_2(F_\xi) \quad (10)$$

where $\mathcal{L}_1$ and $\mathcal{L}_2$ are operators defined by

$$\mathcal{L}_1 = (j\omega\epsilon)^{-1}\left\{k^2 + \frac{\partial^2}{\partial\eta^2}\right\} \quad \text{and} \quad \mathcal{L}_2 = (j\omega\epsilon)^{-1}\left\{\frac{\partial^2}{\partial\eta\partial\xi}\right\}. \quad (11)$$

$F_\eta$ and $F_\xi$ are components of the electric vector potential given by

$$F_\eta = \int\int_{S_1} I_1\, d\eta_0\, d\xi_0 \quad \text{and} \quad F_\xi = \int\int_{S_1} I_2\, d\eta_0\, d\xi_0 \quad (12)$$

where

$$I_1 = f_q^1(\eta_0)[\sin^2(\theta)G_{yy} + \cos^2(\theta)G_{zz}] \quad (13a)$$

$$I_2 = f_q^1(\eta_0)[G_{zz} - G_{yy}]\sin(\theta)\cos(\theta). \quad (13b)$$

Because of the $|z - z_0|$ term in the Green's function and the geometry of the compound slot, the evaluation of $Y^{\text{int}}$ for

the actual slot geometry is very much complicated, as shown below

$$Y_{pq}^{\text{int}} = \int_{-W}^{W} \left\{ \int_{-L}^{\eta'} f_p^1(\eta) H_\eta^{\text{regI}}\, d\eta + \int_{\eta'}^{\eta''} f_p^1(\eta) H_\eta^{\text{regII}}\, d\eta + \int_{\eta''}^{L} f_p^1(\eta) H_\eta^{\text{regIII}}\, d\eta \right\} d\xi \quad (14)$$

where $H_\eta^{\text{regI}}(i = \text{I,II,III})$ are the magnetic fields in the three regions of the slot as shown in Fig. 1(d) which, in turn, however, involve the following integrals:

$$H_\eta^{\text{regI}} = \sum_{i=1}^{2} \mathcal{L}_i \left\{ \int_{-W}^{\xi_0'} \int_{-L}^{\eta_0'} I_i(z > z_0)\, d\eta_0\, d\xi_0 + \int_{-W}^{\xi_0'} \int_{\eta_0'}^{L} I_i(z < z_0)\, d\eta_0\, d\xi_0 + \int_{\xi_0'}^{W} \int_{-L}^{L} I_i(z < z_0)\, d\eta_0\, d\xi_0 \right\} \quad (15a)$$

$$H_\eta^{\text{regII}} = \sum_{i=1}^{2} \mathcal{L}_i \left\{ \int_{-W}^{W} \left\{ \int_{-L}^{\eta_0'} I_i(z > z_0)\, d\eta_0 + \int_{\eta_0'}^{L} I_i(z < z_0)\, d\eta_0 \right\} d\xi_0 \right\} \quad (15b)$$

$$H_\eta^{\text{regIII}} = \sum_{i=1}^{2} \mathcal{L}_i \left\{ \int_{-W}^{\xi_0''} \int_{-L}^{L} I_i(z > z_0)\, d\eta_0\, d\xi_0 + \int_{\xi_0''}^{W} \int_{L}^{\eta_0'} I_i(z > z_0)\, d\eta_0\, d\xi_0 + \int_{\xi_0''}^{W} \int_{\eta_0'}^{L} I_i(z < z_0)\, d\eta_0\, d\xi_0 \right\}. \quad (15c)$$

The argument $(z < z_0)$ and $(z > z_0)$ of $I_i$ indicates that the term $|z - z_0|$ appearing in the Green's function expression should be taken accordingly.

The various limits of integrations appearing in (15a)–(15c) are given below

$$\eta' = -L - (\xi - W)\tan(\theta);\ \eta'' = L - (\xi + W)\tan(\theta)$$

$$\xi_0' = \xi + (L + \eta)\cot(\theta);\ \xi_0'' = \xi + (\eta - L)\cot(\theta)$$

and

$$\eta_0' = \eta + (\xi - \xi_0)\tan(\theta). \quad (16)$$

When the modified geometry of the slot as shown in Fig. 1(b) is used (wherein the narrow edges of the slot are made perpendicular to the $z$ direction), the expression for $Y^{\text{int}}$ is reduced to the following simpler form which is then evaluated analytically:

$$Y_{pq}^{\text{int}} = \int_{-W}^{W} \int_{g_2(\xi)}^{g_1(\xi)} f_p^1(\eta) \sum_{i=1}^{2} \mathcal{L}_i \left\{ \int_{-W} \left\{ \int_{g_2(\xi_0)}^{\eta_0'} I_i(z > z_0)\, d\eta_0 + \int_{\eta_0'}^{g_1(\xi_0)} I_i(z < z_0)\, d\eta_0 \right\} d\xi_0 \right\} \quad (17)$$

where

$$g_1(\xi) = L - \xi\tan(\theta) \quad \text{and} \quad g_2(\xi) = -L - \xi\tan(\theta). \quad (18)$$

### C. Evaluation of $Y^{\text{ext}}$

In the case of dissimilar primary and secondary waveguides, $Y^{\text{ext}}$ is the negative of $Y^{\text{int}}$ evaluated with the corresponding dimensions of the secondary waveguide and the slot offset in the secondary waveguide. When coupling is between identical waveguides, $Y^{\text{ext}}$ is simply the negative of $Y^{\text{int}}$.

### D. Scattering Matrix

The dominant mode-scattering parameters at the center of the slot $(z = 0)$ are found from the knowledge of the dominant mode backscattered field $(E_x^{bs})$ and the forward-scattered field $(E_x^{fs})$ due to the aperture field in $S_1$ in the primary waveguide, and the dominant mode field ($E_x^3$ and $E_x^4$) scattered into ports 3 and 4 by the aperture field in $S_2$, together with the incident field at the center of the slot.

$$S_{11} = E_x^{bs}/E_x^{\text{inc}};\ S_{21} = 1 + (E_x^{fs}/E_x^{\text{inc}})$$

$$S_{31} = E_x^3/E_x^{\text{inc}};\quad \text{and} \quad S_{41} = E_x^4/E_x^{\text{inc}}. \quad (19)$$

The scattering parameters $S_{22}$, $S_{12}$, $S_{32}$, and $S_{42}$ can be found from (19) using the following relations:

$$S_{22}(\delta) = S_{11}(-\delta);\ S_{12}(\delta) = S_{21}(-\delta)$$

$$S_{32}(\delta) = S_{41}(-\delta);\quad \text{and} \quad S_{42}(\delta) = S_{31}(-\delta). \quad (20a)$$

In the case of dissimilar primary and secondary waveguides, the scattering parameters have to be modified suitably as given in [13] to restore the reciprocity property. From the symmetry considerations, the other $S$ parameters can be given as

$$S_{13} = S_{31};\ S_{23} = S_{32};\ S_{33} = S_{11};\ S_{43} = S_{21}$$

$$S_{14} = S_{41};\ S_{24} = S_{42};\ S_{34} = S_{12};\quad \text{and} \quad S_{44} = S_{22}. \quad (20b)$$

### E. Evaluation of Equivalent Network

Unlike the longitudinal slot or transverse slot or the centered inclined slot, $S_{22} \neq S_{11}$ in a compound slot due to the asymmetry of the slot with respect to the $z = 0$ plane (center of the slot). In this context, it is worth evaluating the expression for the loading due to the slot as seen at the $z = 0$ plane of the primary waveguide. A generalized $T$ network is proposed as the equivalent network whose elements $Z_1$, $Z_2$ and $Z_3$ as shown in Fig. 1(e) can be computed from the following expressions:

$$Z_1 = [\{(1 + S_{11})(1 - S_{22}) + S_{21}^2\}/\Delta] - Z_2 \quad (21a)$$

$$Z_3 = [\{(1 - S_{11})(1 + S_{22}) + S_{21}^2\}/\Delta] - Z_2 \quad (21b)$$

$$Z_2 = 2S_{21}/\Delta \quad \text{and} \quad Y_2 = 1/Z_2 \quad (21c)$$

$$\Delta = (1 - S_{11})(1 - S_{22}) - S_{21}^2. \quad (21d)$$

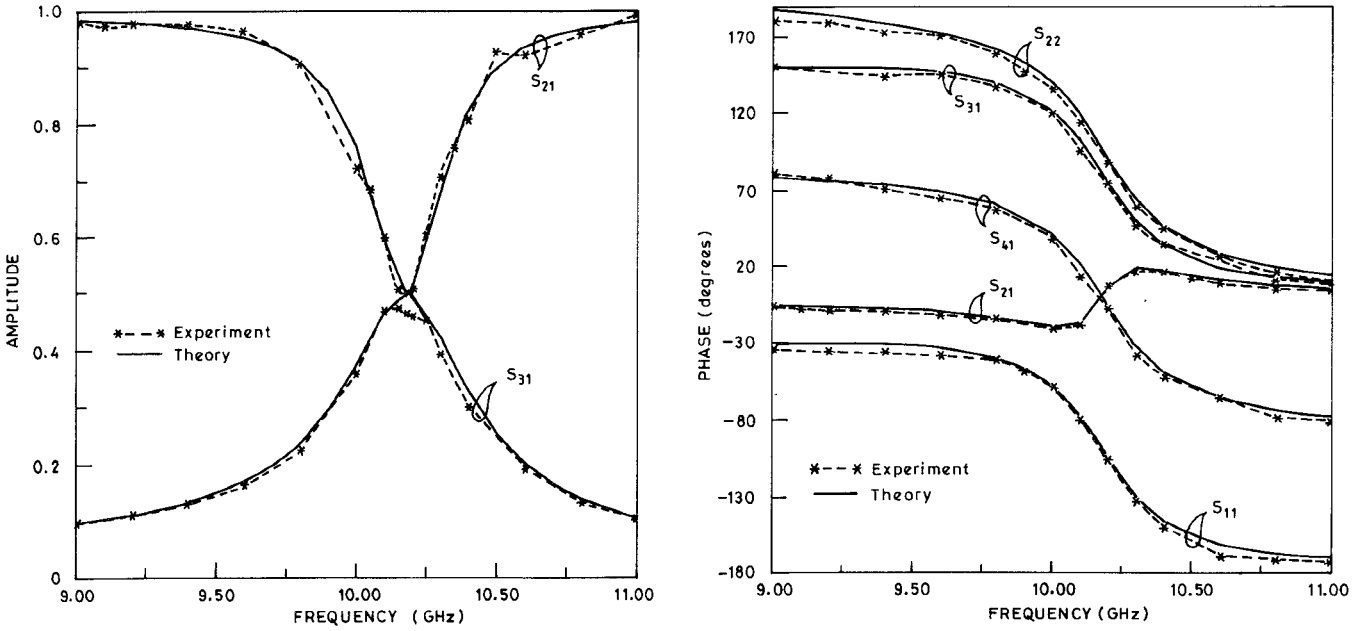


(a) (b)

Fig. 2. Variation of the scattering parameters of compound slot coupler between standard $X$-band waveguides with frequency. $2L = 1.48$ cm, $2W = 0.1$ cm, $\delta = 0.508$ cm, $\theta = 30°$. $a \rightarrow$ amplitude, $b \rightarrow$ phase.

## III. Analysis of Compound Slot Radiator

Removing the secondary waveguide in the compound slot parallel coupler results in a compound slot radiator. In the analysis of compound slot radiator, except $Y^{\text{ext}}$, all of the other matrices remain the same in (5). $Y^{\text{ext}}$ in this case can be evaluated numerically using the half-space Green's function by properly taking into account the singularity using suitable variable transformations as outlined in [14]. The scattering parameters $S_{11}$, $S_{21}$, and $S_{22}$ as well as the equivalent $T$ network can be evaluated in the same manner as that of the compound slot coupler given earlier.

## IV. Numerical and Experimental Results

Following the aforementioned procedure, the $S$ parameters of the compound slot parallel coupler are computed using a computer program which is run on a Cyber 180/840 mainframe computer. Most of the computer time is spent in computing the $Y^{\text{int}}$ and $Y^{\text{ext}}$ matrices. The results are found to converge for $m = 50$ and $n = 50$. The results obtained using three and five basis functions show almost no difference in the amplitude of $S$ parameters, and very little difference on the order of 0.1–0.5° in the phase. The time taken for the computation of $S$ parameters with $m = n = 50$, in the case of identical waveguides, for $N = 3$ is 64 s, whereas for $N = 5$, it is 160 s. In all of the subsequent calculations, $m = n = 50$ and $N = 5$ is used.

The scattering parameters $S_{11}$, $S_{22}$, $S_{21}$, $S_{31}$, and $S_{41}$ are computed for a compound slot parallel coupler between identical waveguides having $a = 1.016$ cm, $b = 2.286$ cm, $2L = 1.48$ cm, $2W = 0.1$ cm, $\theta = 30°$, $\delta = 0.507$ cm, and $t = 0.127$ cm over a frequency range of 9.0–11.0 GHz. The scattering coefficients have also been measured using an HP 8410C Network Analyzer setup. Since the amplitudes of $S_{11}$, $S_{22}$, $S_{31}$, and $S_{41}$ are almost equal, the theoretical and experimental results for $|S_{31}|$ and $|S_{21}|$ are presented in Fig. 2(a), and the phase of $S_{11}$, $S_{22}$, $S_{21}$, $S_{31}$, and $S_{41}$ are presented in Fig. 2(b).

TABLE I

| $\delta$ | 0.0 | | 0.127 cm | | 0.381 cm | | 0.635 cm | |
|---|---|---|---|---|---|---|---|---|
| $\theta$ (deg) | $Z_2=Z_1$ | $Y_2$ | $Z_2=Z_1^*$ | $Y_2$ | $Z_2=Z_1^*$ | $Y_2$ | $Z_2=Z_1^*$ | $Y_2$ |
| 0 | | | j 136E-3 | 2 0 | j 12E-2 | 2 0 | j 3251-2 | 2 0 |
| 5 | 2 | 0 | j0 619 | 1 44 | j0 1884 | 1 93 | j0 088 | 1 98 |
| 10 | 2 | 0 | j1 235 | 0.792 | j0 378 | 1.748 | j0.181 | 1 933 |
| 15 | 2 | 0 | j1.85 | 0 453 | j0.566 | 1 513 | j0 273 | 1 857 |
| 20 | 2 | 0 | j2.459 | 0.284 | j0.7529 | 1.275 | j0.36 | 1 76 |
| 25 | 2 | 0 | j3 07 | 0 192 | j0 94 | 1.062 | j0 455 | 1 65 |
| 30 | 2 | 0 | j3 69 | 0 137 | j1.129 | 0 88 | j0 545 | 1 54 |
| 35 | 2 | 0 | j4 33 | 0 101 | j1 324 | 0 728 | | |
| 40 | 2 | 0 | j5 0 | 0.077 | j1 531 | 0 6 | | |
| 45 | 2 | 0 | j5 76 | 0 059 | j1 759 | 0 49 | | |

( - $Z_2=Z_1$ at $\theta = 0°$ for all $\delta$)

Fig. 3(a) and (b) give the variation of the phase of resonant $S_{11}$ and resonant length ($2L_{\text{res}}$), respectively, with slot inclination for offsets $\delta = 0$, 0.127, 0.381, 0.635 cm (0, 0.05, 0.15, 0.25 in) with $a = 1.016$ cm, $b = 2.286$ cm, $2W = 0.1$ cm, $t = 0.127$ cm at $f = 9.375$ GHz.

The equivalent $T$ network as shown in Fig. 1(e) of the above coupler at $f = 9.375$ GHz for various inclinations of the slot and offset is found and given in Table I.

The variation of resonant length and magnitude of resonant $S_{11}$ with offset is computed for a compound slot radiator having $a = 1.016$ cm, $b = 2.286$ cm, $2W = 0.156$ cm, $t = 0.127$ cm at $f = 9.3$ GHz for $\theta = 0°$ and 20°. The results are compared with the corresponding curves in [15, Figs. 6 and 9]. The data are presented in Fig. 4(a) and (b), respectively.

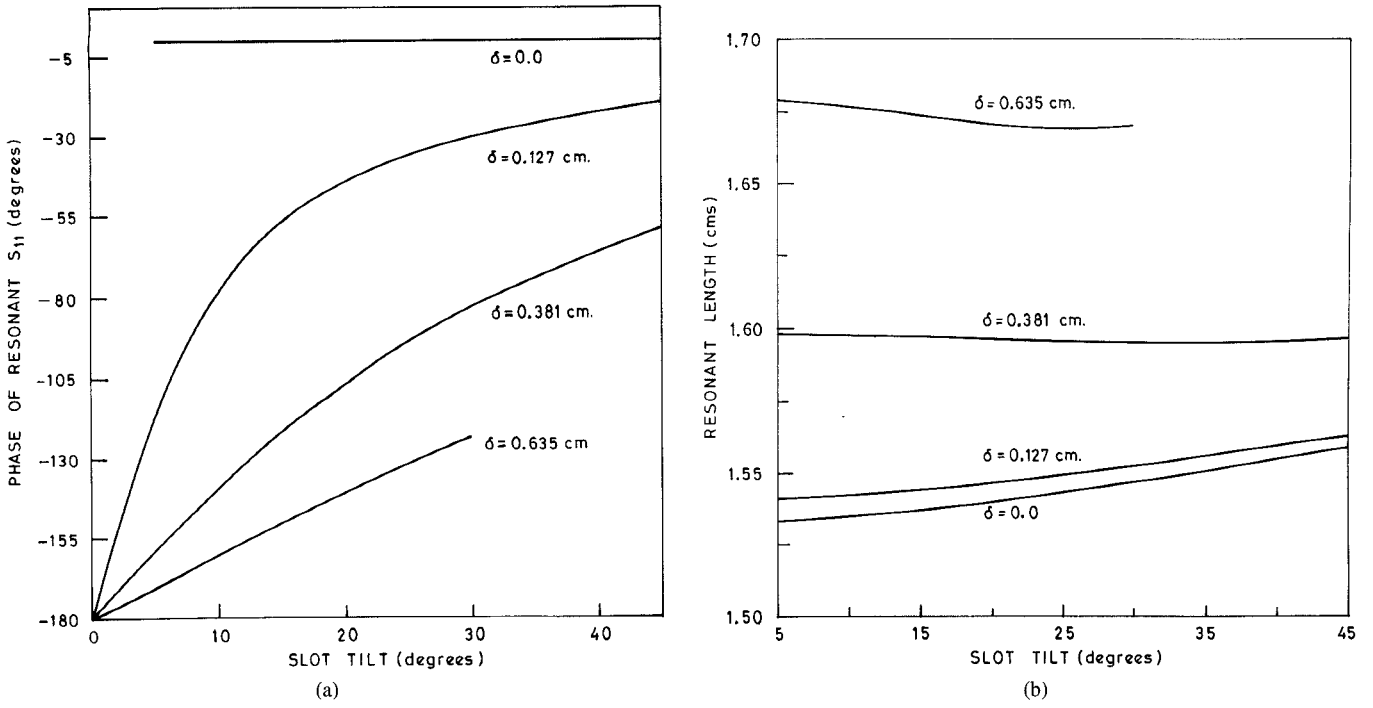


Fig. 3. (a) Variation of the phase of resonant $S_{11}$ of compound slot coupler between parallel $X$-band waveguides with inclination and offset at $f = 9.375$ GHz with $2W = 0.1$ cm. (b) Variation of the resonant length in a compound slot coupler between parallel $X$-band waveguides with inclination and offset at $f = 9.375$ GHz with $2W = 0.1$ cm.

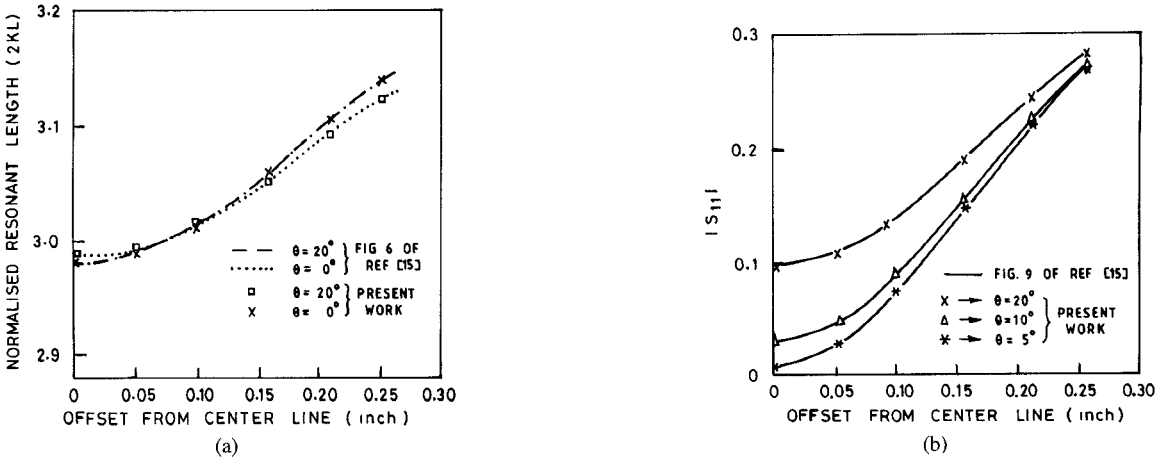


Fig. 4. (a) Variation of normalized resonant length of compound radiating slot in standard $X$-band waveguide. $2W = 0.15875$ cm, $f = 9.3$ GHz. (b) Variation of magnitude of resonant $S_{11}$ in a compound slot radiator in standard $X$-band waveguide. $2W = 0.15875$ cm, $f = 9.3$ GHz.

Plotted in Fig. 5(a) is the variation of the phase of aperture electric field at resonance, obtained from the $[B]$ matrix (6f), over a wide range of angles for a compound slot radiator having $a = 1.016$ cm, $b = 2.286$ cm, $2W = 0.156$ cm, $t = 0.127$ cm at $f = 9.3$ GHz for $\delta = \pm 0.254$ cm, and $\pm 0.508$ cm.

The equivalent $T$ network of the above compound slot radiator at resonance is evaluated for various inclinations at $f = 9.3$ GHz for $\delta = +0.254$ cm and $+0.508$ cm. The values of series reactances $X_1$ and $X_3$ and shunt conductance $G_2$ are plotted in Fig. 5(b). The series resistances $R_1$ and $R_3$ and shunt susceptance $B_2$ are almost equal to zero at resonance.

## V. Discussion

This paper has described a rigorous analysis of a parallel waveguide coupler coupled through a wide inclined and offset slot in the common broad wall between the waveguides. The method of moments has been applied in conjunction with global sinusoidal basis functions and Galerkin's technique to solve the pertinent coupled integro-differential equations. The complexity in the analysis is reduced by a novel modification of the slot geometry, thereby enabling the complete analytical evaluation of the integrals involved. It is imperative, in this context, to point out that this modification results in a poor approximation at large angles of inclination of the slot from

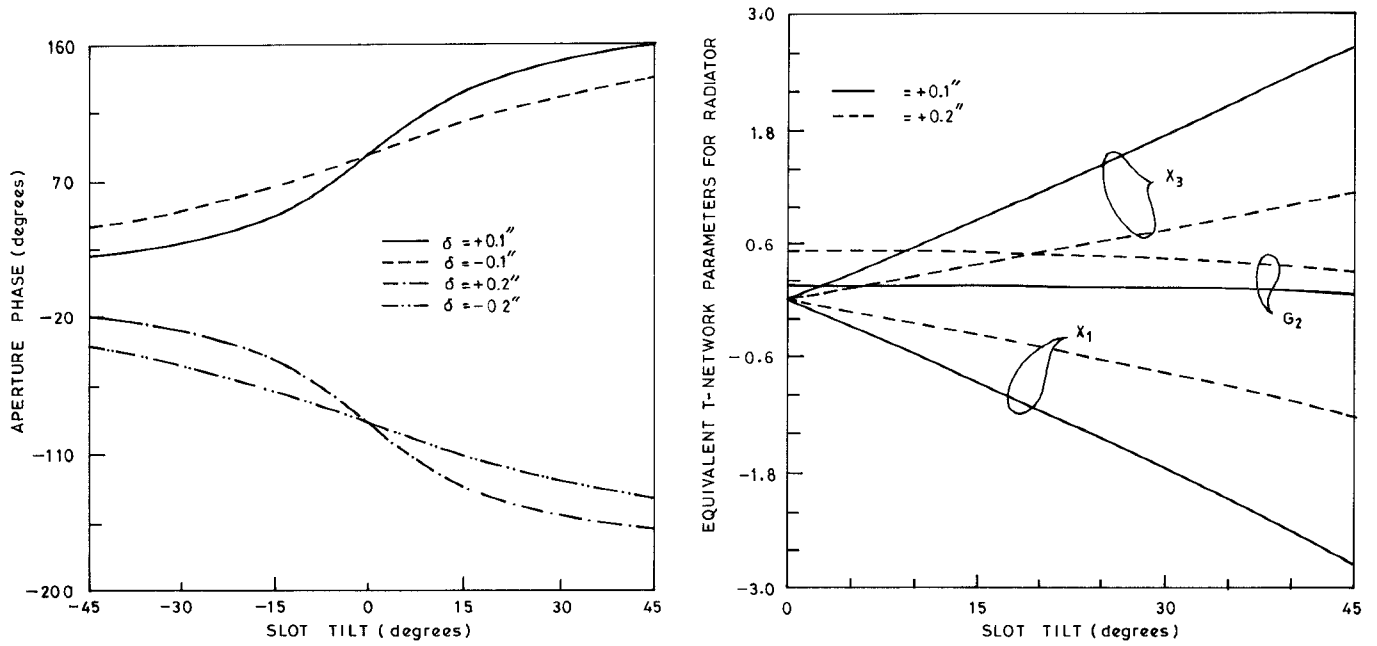


Fig. 5. (a) Variation of phase of the slot aperture electric field at resonance with slot inclination for a compound slot radiator in a standard $X$-band waveguide for various offsets ($\delta$). $2W = 0.156$ cm, $f = 9.3$ GHz. (b) Variation of resonant $T$-equivalent network parameters with inclination of a compound radiating slot in a standard $X$-band waveguide. $2W = 0.156$ cm, $f = 9.3$ GHz.

the axis of the waveguide. However, large angles of inclination of the slot are seldom needed in parallel couplers or radiators; hence, this modification is very helpful in analyzing compound slots in parallel couplers and radiators.

The excellent agreement between the theoretical and experimental results shown in Fig. 2(a) and (b) justifies the validity of this method. The study of resonant coupling and the reflection coefficient in the case of a parallel coupler between identical waveguides has shown some interesting results. Unlike the case of the compound slot cross coupler [11], here the magnitude of resonant coupling and the reflection coefficient have shown no variation with either offset or inclination, and are all found to be identical and equal to a value of 0.5, which is tantamount to 6-dB coupling to all four ports. This phenomenon has been observed earlier by Datta *et al.* [13] in the case of a longitudinal slot parallel coupler between identical waveguides, which is a special case of the present case, and also in the compound slot cross coupler [11] when $\theta = 45°$, in which case the slot orientation in both the main and branch waveguides becomes identical.

The magnitudes of the $S$ parameters are found to be independent of the feeding ports (either port 1 or 2), whereas the phases of the corresponding parameters differ. In general, for a parallel coupler between identical waveguides, the following relations hold: $\angle S_{11}(\theta) = -\angle S_{11}(-\theta)$; $\angle S_{21}(\theta) = \angle S_{12}(\theta)$; $\angle S_{41}(\theta) = \angle S_{32}(\theta)$; $\angle S_{31}(\theta) = \angle S_{42}(-\theta)$; $\angle S_{11} = \angle S_{31} \pm 180°$; $\angle S_{41} = \angle(1 - S_{21}) \pm 180°$. At resonance, the complete $S$ matrix of the parallel coupler between identical waveguides can be given as a function of the phase of $S_{11}$ ($r = e^{j\psi}$ where $\psi = \angle S_{11}$) alone, as shown below:

$$[S] = 0.5 \begin{bmatrix} r & 1 & -r & 1 \\ 1 & r^* & 1 & -r \\ -r & 1 & r & 1 \\ 1 & -r^* & 1 & r^* \end{bmatrix}.$$

Fig. 3(a) gives the typical variation of the phase of resonant $S_{11}$. Unlike the longitudinal or transverse slot or centered slot, the phase of resonant $S_{11}$ and $S_{22}$ (which are not equal in the compound slot case) varies with tilt and offset of the slot, rendering it impossible to be represented by a simple shunt or series element. As seen from Fig. 3(b), the resonant length is relatively insensitive to inclination compared to offset.

The equivalent network evaluation (as presented in Table I) has shown that the compound slot parallel coupler behaves like an antisymmetric ($Z_1 = Z_3^*$) $T$ network. At resonance, the series elements ($Z_1$ and $Z_3$) are purely reactive and the shunt element ($Y_2$) is purely conductive. Away from resonance, all of the elements have complex values. Also, the series elements have to be interchanged when either $\theta$ or $\delta$ is negative. However, at $\delta = 0$, $Y_2 = 0$ and $Z_1 = Z_2$, i.e., the centered inclined slot behaves as a series element, and at resonance, $Z_1 = Z_2 = 1$, independent of inclination.

For the sake of comparison of the present method with the available literature [15], the analysis of a coupler is extended to a radiator. Fig. 4(a) and (b) show good agreement between the results obtained using the present method and those reported in the literature [15]. Also, quantitative results for the variation of the phase of aperture electric field with $\theta$ and $\delta$ [as shown in Fig. 5(a)] can be used to obtain a shaped beam pattern.

Equivalent network representation of a compound slot radiator [Fig. 5(b)] shows it as an antisymmetric $T$ network

wherein the series reactances (impurities to the shunt element) are not clearly negligible (even at resonance), as opposed to the conclusion made by Rengarajan as just a series or shunt element [12, sec. IV]. Our finding corroborates the suggestion given in [16] that a compound slot radiator can be represented by an antisymmetric $T$ network.

Results computed using this method for the coupler have shown excellent agreement with experimental results. Results computed using this method for the radiator have shown very good agreement with those available in the literature. The modified geometry of the compared slot will be very helpful to study the multiaperture coupler or an array (taking the mutual coupling effects into account) in reducing the analytical as well as computational effort drastically.

## REFERENCES


[1] H. A. Bethe, "Theory of diffraction by slots," *Phys. Rev.*, vol. 66, pp. 163–182, 1944.

[2] S. B. Cohn, "Microwave coupling by large apertures," *Proc. IRE*, vol. 40, pp. 696–699, 1952.

[3] R. Levy, "Improved single and multiaperture waveguide coupling theory, including explanation of mutual interaction," *IEEE Trans. Microwave Theory Tech.*, vol. MTT-28, pp. 331–338, 1980.

[4] W. H. Watson, *The Physical Principles of Waveguide Transmission and Antenna Systems.* London: Clarendon, 1949.

[5] A. J. Sangster, "Variational method for the analysis of waveguide coupling," *Proc. IEE*, vol. 112, pp. 2171–2179, Dec. 1965.

[6] V. M. Pandharipande and B. N. Das, "Coupling of waveguides through large apertures," *IEEE Trans. Microwave Theory Tech.*, vol. MTT-26, pp. 209–212, Mar. 1979.

[7] T. V. Khac, "Studies on slot discontinuities in rectangular waveguides," Ph.D. dissertation, Monash Univ., Australia, Nov. 1974.

[8] S. N. Sinha, "A generalized network formulation for a class of waveguide coupling problems," *Proc. IEE*, pt. H, vol. 134, pp. 502–508, Dec. 1987.

[9] S. R. Rengarajan, "Characteristics of longitudinal transverse coupling slot in crossed rectangular waveguides," *IEEE Trans. Microwave Theory Tech.*, vol. 37, pp. 1171–1177, Aug. 1989.

[10] ——, "Analysis of a centered-inclined waveguide slot coupler," *IEEE Trans. Microwave Theory Tech.*, vol. 37, pp. 884–889, May 1989.

[11] ——, "Compound coupling slots for arbitrary excitation of waveguide fed planar slot arrays," *IEEE Trans. Antenn. Propagat.*, vol. 38, pp. 276–280, Feb. 1990.

[12] S. R. Rengarajan and A. G. Derneryd, "Application of compound coupling slots in the design of shaped beam antenna patterns," *IEEE Trans. Antenn. Propagat.*, vol. 41, pp. 59–65, Jan. 1993.

[13] A. Datta, A. M. Rajeek, A. Chakraborty, and B. N. Das, "S matrix of a broad wall coupler between dissimilar rectangular waveguides," *IEEE Trans. Microwave Theory Tech.*, accepted for publication.

[14] D. Satyanarayana and A. Chakraborty, "Analysis of wide inclined slot coupled narrow wall coupler between dissimilar rectangular waveguides," *IEEE Trans. Microwave Theory Tech.*, May 1994.

[15] S. R. Rengarajan, "Compound radiating slots in a broad wall of a rectangular waveguide," *IEEE Trans. Antenn. Propagat.*, vol. 37, pp. 1116–1123, Sept. 1989.

[16] ——, "Compound broad-wall slots for array applications," *IEEE AP Mag.*, vol. 32, pp. 20–26, Dec. 1990.

[17] A. Datta, "Studies on collinear longitudinal broad wall slot array and its feed," Ph.D. dissertation, Indian Inst. Technol., Kharagpur, 1992.

[18] R. W. Lyon and A. J. Sangster, "Efficient moment method analysis of radiating slots in a thick walled rectangular waveguide," *Proc. IEE*, pt. H, vol. 128, pp. 197–205, Aug. 1981.


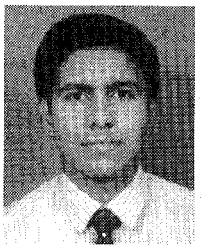

**A. Mohammed Rajeek** was born in Tirunelveli District, TamilNadu, India, on May 25, 1971. He received the B.E. degree in electronics and communication engineering from the College of Engineering, Guindy, Anna University, Madras, India, in 1992, and the M.Tech. degree in microwave engineering from the Indian Institute of Technology, Kharagpur, in 1993.

He is presently a research scholar at IIT. His fields of interest include numerical modeling of waveguide junctions, and numerical methods as applied to microwave circuits and antennas.

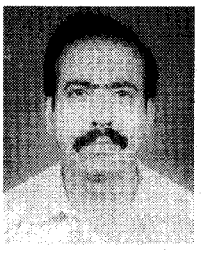

**Ajay Chakraborty** (A'87–SM'90) received the B.Tech, M.Tech., and Ph.D. degrees from the Indian Institute of Technology, Kharagpur, in 1975, 1977, and 1982, respectively.

He joined the faculty of the E&ECE Department at IIT Kharagpur in 1980. He worked as a visiting assistant professor at Syracuse University from Aug. 1989 to May 1990. His current research interests are antenna pattern synthesis, slot arrays, feednetworks for phased arrays, and ESD studies. Currently, he is a professor in the E&ECE Department at the Indian Institute of Technology, Kharagpur.